POLITECNICO DI TORINO
Repository ISTITUZIONALE

Cognitive and autonomous QoT-driven optical line controller

(Article begins on next page)

10 April 2024

Cognitive and autonomous QoT-driven optical line controller

Giacomo Borraccini,[1,*] ● **Andrea D'Amico,**[1] ● **Stefano Straullu,**[2]
Antonino Nespola,[2] **Stefano Piciaccia,**[3] **Alberto Tanzi,**[3] **Gabriele Galimberti,**[3]
Stefano Bottacchi,[4] **Scott Swail,**[4] **and Vittorio Curri**[1] ●

[1]*Department of Electronics and Telecommunications, Politecnico di Torino, Corso Duca degli Abruzzi 24, Torino (TO) 10129, Italy*
[2]*LINKS Foundation, via Pier Carlo Boggio 61, Torino (TO) 10138, Italy*
[3]*Cisco Photonics, via S. M. Molgora, 48/C, Vimercate (MI) 20871, Italy*
[4]*Lumentum Operations LLC, 1001 Ridder Park Drive, San Jose, California 95131, USA*
Corresponding author: giacomo.borraccini@polito.it

In the direction of disaggregated and cognitive optical networks, this work proposes and experimentally tests a vendor-agnostic optical line controller architecture capable of autonomously setting the working point of optical amplifiers to maximize the capacity of a ROADM-to-ROADM (reconfigurable optical add–drop multiplexer) link. From a procedural point of view, once the equipment is installed, the presented software framework performs an automatic characterization of the line, span by span, to abstract the properties of the physical layer. This process requires the exploitation of monitoring devices such as optical channel monitors and optical time domain reflectometers, available, in a future perspective, in each amplification site. On the basis of this information, an optimization algorithm determines the working point of each amplifier to maximize the quality of transmission (QoT) over the entire band. The optical line controller has been experimentally tested in the laboratory using two different control strategies, achieving in both cases a homogeneous QoT for each channel close to the maximum average and an excellent match with respect to emulation results. In this framework, the Gaussian noise simulation in Python (GNPy) open source Python library is used as the physical model for optical propagation through the fiber, and the covariance matrix adaptation evolution strategy is used as an optimization algorithm to identify properties of each fiber span and to maximize the link capacity. © 2021 Optical Society of America under the terms of the [OSA Open Access Publishing Agreement](https://doi.org/10.1364/JOCN.424021)

https://doi.org/10.1364/JOCN.424021

1. INTRODUCTION

Driven by the increasing and greedy Internet data traffic request [1], optical network operators are working to satisfy this need, improving the already installed resources, or updating them thanks to the introduction of new technological discoveries [2]. In this context, the most relevant support for service capacity increase and system management is conferred by optical network automation [3], due to standardization [4,5] and the consequent implementation of software-defined (SD) networks [6–8]. Another important characteristic for an efficient usage of optical networks is the capability of the infrastructure to be agnostic with respect to the adopted vendor equipment, also favoring a more rapid deployment and the integration of new functions [9]. Definitely, this is allowed by hardware and software disaggregation [10–12], pushing in the direction of cognitive optical networks [13].

Starting from the last decade, cognition has been introduced and theorized as an emerging feature of the next generation of optical networks [14]. Cognition implies the autonomous and

prompt control of a network at each abstraction layer operating decisions and strategies based on the processing of information related to the status of the system [15]. The response to the increasing complexity of the infrastructure is given by the possibility to probe the condition of the network through monitoring devices and to efficiently analyze the extracted information using flexible software modules [16]. In this scenario, telemetry and monitoring devices cover a fundamental role, since they make it possible to retrieve information from the field to address different tasks and operations [17].

Our investigation has the purpose to deepen cognition in optical networks at the physical layer, defining a vendor-agnostic optical line controller (OLC) architecture capable of autonomously setting the working point of optical amplifiers to maximize the capacity of the optical link. The presented framework is based on an automatic characterization procedure of the line, span by span, to abstract the properties of the physical layer, exploiting the monitoring devices present in each amplification site such as optical channel monitors (OCMs) and optical time domain reflectometers (OTDRs).

On the basis of this information, an optimization algorithm determines the working point of each amplifier to obtain the highest and flattest quality of transmission (QoT) for each channel. The entire system has been experimentally tested in the laboratory using two different optimization strategies, showing interesting behaviors and an excellent match with respect to emulation results. The main tools used within the framework are the Gaussian noise simulation in Python (GNPy) open source Python library, used as a physical model for optical propagation through the fiber, and the covariance matrix adaptation evolution strategy (CMA-ES), used as an optimization algorithm to identify properties of each fiber span and to maximize the link capacity. The conceived formalism is independent of the adopted physical model or optimization algorithm, allowing the determination of the set of physical properties captured by the telemetry.

The authors have already presented in previous works the application of these methodologies on a laboratory experimental setup. In particular, [18] provides the validation of the physical layer characterization procedure feeding the GNPy physical model with the extracted physical layer description and verifying the match in the optical propagation between emulation and measurements. In [19], the QoT-driven optimization approach is applied on a real optical line given the physical layer description of each fiber span. This work fully describes an example of automation of an optical line starting from the equipment installation until the determination of the optimal amplifier working point. We provide the complete mathematical formulation of each optimization methodology, defining two different QoT-driven optimization problems to maximize the capacity of the line and comparing them in terms of achieved performance.

The body of the paper is divided into four main sections. In Section 2, we contextualize the developed system from a network point of view, describing the actors, their behaviors, and the interactions on which they are based. In Section 3, we present the complete optimization methodology used for both the physical layer characterization procedure and optical line control, describing the optimization problem according to three main aspects: the physical model, the optimization algorithm, and the problem formulation. Regarding the latter, we propose two different control strategies based on global optimization, evaluating QoT degradation at the optical line output, and on a local optimization that analyzes the working point of each amplifier. In Section 4, the experimental setup used to test the developed OLC is presented, providing technical details and explanations related to measurement precautions. In Section 5, we report and discuss the experimental results of both physical layer characterization and optical line control, focusing on the comparison between the two proposed control strategies.
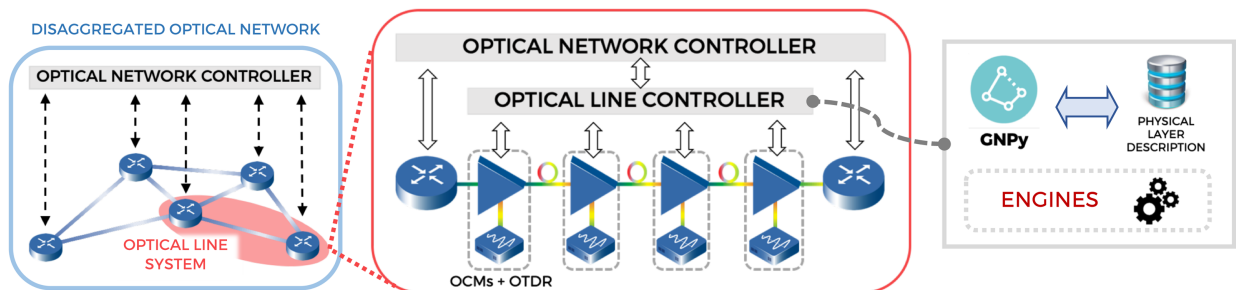
2. OPTICAL NETWORK ARCHITECTURE

Considering a disaggregated optical network within a SD networking (SDN) framework, we assume that the operations among each reconfigurable optical add–drop multiplexer (ROADM) node are managed and orchestrated by an optical network controller (ONC) (Fig. 1). Both ROADM nodes, which are constituted by transmission-technology-agnostic disaggregated ROADMs [20,21], and amplified wavelength division multiplexed (WDM) optical line systems (OLSs) [22–24] can operate in a completely disaggregated manner. Each OLS connecting two adjacent ROADM nodes refers to an OLC that in turn communicates with the ONC. Focusing on the C-band transmission scenario, each OLS is composed of a sequence of amplification sites and fiber spans. Each amplification site is constituted by an erbium-doped fiber amplifier (EDFA) and integrated monitoring devices at both amplifier terminals, while a single fiber span includes a certain number of fiber spools connected by mechanical connectors. The management of each amplifier operated by the OLC consists of collecting feedback from the monitoring devices regarding the local status of the propagating spectrum and setting the working point according to a specific ONC request. On the basis of the latter, the OLC can apply a control strategy relying on a physical model of the optical propagation, allowing the estimation of the QoT (in particular, in this investigation, we use GNPy [25] for this purpose), and a physical layer description of the in-field equipment.

It is widely demonstrated that the use of coherent optical technologies makes it possible to define the generalized signal-to-noise ratio (GSNR) as a valid figure of merit for the QoT [26], enabling the abstraction of the optical propagation performance of a specific lightpath. Modeling the latter as an additive white Gaussian noise (AWGN) nonlinear channel, the corresponding GSNR degradation can be expressed using the following formula:

$$\text{GSNR} = \frac{P_{ch}}{P_{\text{ASE}} + P_{\text{NLI}}}, \tag{1}$$

where P_{ch} is the average signal power, and P_{ASE} and P_{NLI} represent the noise contributions due to the amplified spontaneous emission (ASE) introduced by each amplification system and due to the nonlinear interference (NLI) impairment

Fig. 1.   Softwarized architecture of the physical layer aware OLS within the context of a SDN disaggregated optical transport network.

generated by each fiber span. So, the OLS controller covers a fundamental role whose goal can be mathematically formulated as the equal distribution and maximization of the QoT optimizing the working point of amplifiers. This optimization process can be significantly improved by a more faithful and accurate physical layer description. In this framework, the automation of the physical layer characterization is enabled by the exploitation of telemetry and monitoring devices, probing the properties of each fiber span composing the OLS. Actually, these elements present the highest uncertainty in terms of physical parameters, as the loss coefficient function, effective area, and connector losses, bringing the system to work in an unwanted working point if not properly estimated. The most relevant advantage of this approach is related to the possibility to completely automatize the management of the OLS due to the high flexibility conferred by the described network architecture.

3. OPTIMIZATION METHODOLOGY

In this section, the optimization problems related to the physical layer characterization and amplifier gain control are mathematically formalized, describing all the necessary details that allow adoption of the proposed OLC within a generic scenario. To define without ambiguity each optimization process, the formalism is divided into three subsections: the physical model, the optimization algorithm, and the problem formulation. Both the optimization problems adopt the same physical model and optimization algorithm within a completely different problem formulation.

A. Physical Model

In the presented software framework, the GNPy open source Python library [27,28] is used as the physical model for QoT estimation (QoT-E). The emulation of the optical propagation through a single fiber span or through a complete OLS is performed abstracting three main classes, where each of them is defined by a set of parameters:

1. **Optical fiber**:

   - length, L_S;
   - lumped losses, $l(z)$, located at a specific spacial coordinate, where at least the losses due to the input, $l(0)$, and the output connector, $l(L_S)$, of the fiber span are assumed by default;
   - loss coefficient function, $\alpha(f)$, resolute in frequency;
   - Raman efficiency, $C_R(\Delta f)$;
   - chromatic dispersion, D.

2. **Optical amplifier** (EDFA):

   - mean gain, $\bar{G}$;
   - gain tilt, T.

3. **Input WDM comb**, in which each channel is described by:

   - frequency, f_i, where i is the channel ordinal number within the specified grid that goes from one to the number of channels, N_{ch};
   - baud rate, R_S;

- signal power, $P_{ch}(f_i)$;
- ASE power, $P_{ASE}(f_i)$;
- NLI power, $P_{NLI}(f_i)$.

Defining a certain input WDM comb and a sequence of fibers and amplifiers, these objects make it possible to propagate the spectral information and to compute the status of the WDM comb at the corresponding output. In the developed optimization frameworks, we are interested in the propagation of both the signal power, $P_{ch}(f)$, and the two noise power contributions, $P_{ASE}(f)$ and $P_{NLI}(f)$, with the properties of each element fixed. Consequently, it is possible to operate a QoT-E computing the GSNR for each declared channel in the propagating WDM comb. The main nonlinear effects considered within the calculation of the fiber optical propagation are the inter-channel stimulated Raman scattering (SRS) [29] and the NLI impairment. Regarding the optical amplifier, we define an object that applies to the input WDM comb a gain profile resolute in frequency, $G(f)$, and introduces a quantity of ASE noise proportional to a flat noise figure (NF), providing a specific couple of mean gain, $\bar{G}$, and gain tilt, T. This approach requires an experimental characterization step of the optical amplifier, which is explained in the section related to the experimental setup.

B. Optimization Algorithm

Since in the following study every optimization problem presents a high order of computational complexity from the physical model point of view and a considerable number of variables, we use a stochastic optimization algorithm based on an evolutionary strategy. In particular, the CMA-ES [30,31] is used as an optimization algorithm to identify both properties of each fiber span and to maximize the OLS capacity. This choice is made because the use of optimization algorithms based on evaluation of the objective function gradient is not effective in the case of a high number of variables and irregular problem spaces. In addition, when there are more than two variables to optimize, the estimation of the goodness of the found solution evaluating the shape of the problem space around the optimum is not trivial and is a resource-consuming procedure, regardless of the optimization algorithm.

C. Problem Formulation

In this section, we provide details regarding the mathematical formulation of two different optimization problems that address the physical layer characterization of each fiber span and the amplifier working point design. First, the measurement operative steps of monitoring devices are described to retrieve the required information from the in-field apparatus. Then, the optimization procedure is explained exploiting the telemetry data.

First, we describe the generic OLS scheme on which the optimization methodology is applied. Starting with Fig. 2, the OLS between two adjacent nodes of the optical network is considered as a sequence of N_S spans ended by a single pre-amplifier, where each span is composed of a coupled amplifier–fiber. We assume that each optical amplifier has on-board integrated telemetry and monitoring equipment.
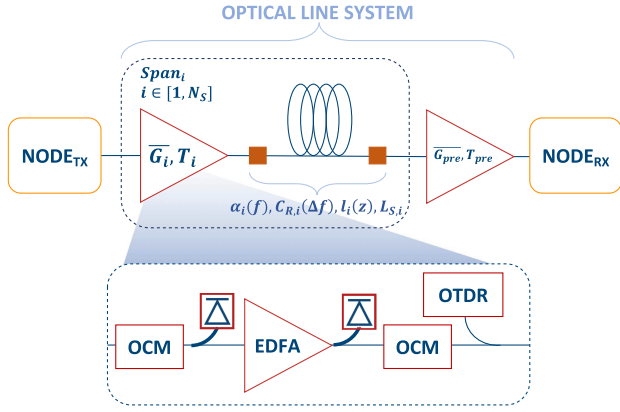
Fig. 2.   General structure of the OLS under investigation.

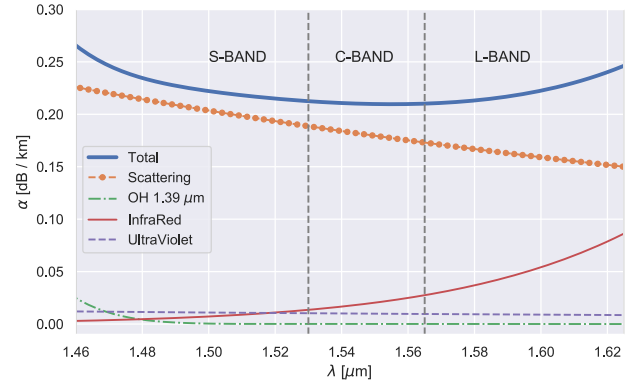**Fig. 3.**   Generic loss coefficient profile and the related four model contributions.

In particular, a single amplification site is equipped with an OCM and a photodiode at both terminals of the EDFA and with an OTDR. The latter performs an analysis on the fiber following the amplifier evaluating the length, the position of lumped losses, and the loss coefficient at the frequency of the OTDR optical pulse $\alpha(f_{\text{OTDR}})$. Regarding the measurement of the propagating spectrum, each OCM retrieves the spectral information resolute in frequency, while integrated photodiodes allow the measurement of the total power minimizing the uncertainty due to eventual lumped losses. This specific amplifier architecture is chosen to perform cognition and automation on the OLS trying to achieve high model accuracy with respect to the experimental outcome.

1. Physical Layer Characterization

This optimization problem is conceived as an initial automatic probing step after the installation and configuration of the OLS hardware equipment and before actual transmission operations, enlarging the physical layer information and making it possible to determine with higher accuracy the amplifier working point definition. From a practical point of view, this procedure can be applied in parallel to each single fiber span, speeding up the OLS characterization process.

First, an OTDR analysis is performed for each fiber span, measuring the fiber span length, L_S, the positions of eventual in-line lumped losses, and estimating the loss coefficients at the pulse frequency, $\alpha(f_{\text{OTDR}})$. Then, excluding the pre-amplifier, each amplifier is set in ASE mode, providing at the corresponding output a C-band ASE full spectrum. The latter is measured by OCMs at both terminals at each fiber span for two different ASE power levels, obtaining four different power profiles: $P^{\text{LOW}}(f, 0)$, $P_{\text{tar}}^{\text{LOW}}(f, L_S)$, $P^{\text{HIGH}}(f, 0)$, $P_{\text{tar}}^{\text{HIGH}}(f, L_S)$. The first measurement at low ASE power is performed to minimize the Raman cross talk contribution, and the second one is done at a higher ASE power level enhancing the inter-channel SRS. The definitions of the two ASE power levels are related to the installed equipment and to the telemetry sensitivity.

Once the OTDR and OCM measurements are available, the fiber span characterization is carried out for each fiber span, aiming to estimate the physical layer parameters able to accurately emulate the experimental behavior using the previously described physical model. A set of parameters for a single fiber

span includes the Raman efficiency scale factor (the normalized profile is assumed), C_R; the loss coefficient function, $\alpha(f)$; the input, $l(z=0)$, and output connectors, $l(z=L_S)$; and the eventual lumped losses detected by the OTDR, $l(0 < z < L_S)$.

Regarding the loss coefficient function, $\alpha(f)$, we use a phenomenological model that considers all the attenuation effects involved in the optical fiber propagation within the frequency range of interest. Starting from [32], we derive the following simplified model in logarithmic units (dB/km) for C-band scenarios:

$$\alpha(\lambda) \simeq \alpha_S(\lambda) + \alpha_{\text{UV}}(\lambda) + \alpha_{\text{IR}}(\lambda) + \alpha_{13}(\lambda), \qquad \textbf{(2)}$$

where

$$\alpha_S(\lambda) = A\lambda^{-4} + B,$$

$$\alpha_{\text{UV}}(\lambda) = K_{\text{UV}}e^{C_{\text{UV}}/\lambda},$$

$$\alpha_{\text{IR}}(\lambda) = K_{\text{IR}}e^{-C_{\text{IR}}/\lambda},$$

$$\alpha_{13}(\lambda) = A_1\left(\frac{A_a}{A_1}e^{\frac{-(\lambda-\lambda_a)^2}{2\sigma_a^2}} + \frac{1}{A_1}\sum_{i=1}^{3}A_ie^{\frac{-(\lambda-\lambda_i)^2}{2\sigma_i^2}}\right)$$

are the Rayleigh scattering, ultraviolet, infrared, and OH⁻ peak absorption contributions, respectively. An example of the total $\alpha(\lambda)$ and its separate contributions is shown in Fig. 3. The Rayleigh scattering impact is linear, the ultraviolet and infrared absorption contributions have exponential forms, and the OH⁻ peak absorption term, centered at 1.39 μm, can be expressed as a quadruple-Gaussian equation. Since the ultraviolet absorption has a constant trend within a frequency range far larger than the only C-band, this term is taken into account, but it is not optimized. As a consequence, Eq. (2) makes it possible to easily derive even broadband loss coefficient functions defining only four parameters: A, B, K_{IR}, and A_1.

The final list of variables to optimize for a single fiber span physical layer characterization is

- Raman efficiency, C_R;
- loss coefficient function, $\alpha(f)$, defined by four parameters: A, B, K_{IR}, and A_1;
- input connector loss, $l(z=0)$;
- output connector loss, $l(z=L_S)$;
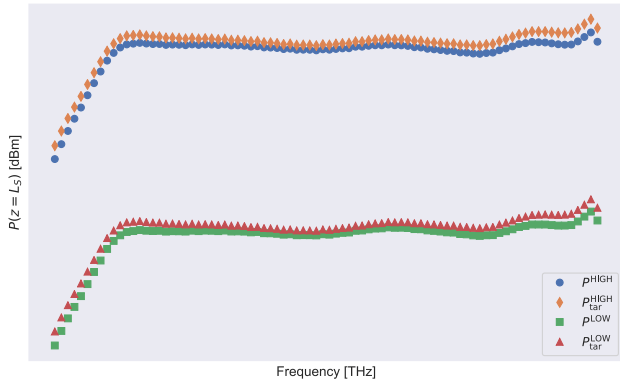
Fig. 4. Adopted metrics for the physical layer characterization procedure, span by span.

Fig. 5. Adopted metrics for *global* GSNR optimization within the optical line control strategy.

- eventual intermediate lumped losses along the fiber span, $l(0 < z < L_S)$.

The objective function to minimize is expressed by the following formula:

$$f(x) = \sqrt{\sum_{i=1}^{N_{\text{SAMPLE}}} \left(P_{\text{tar}}^{\text{LOW}}(f_i, L_S) - P^{\text{LOW}}(f_i, L_S) \right)^2}$$
$$+ \sqrt{\sum_{i=1}^{N_{\text{SAMPLE}}} \left(P_{\text{tar}}^{\text{HIGH}}(f_i, L_S) - P^{\text{HIGH}}(f_i, L_S) \right)^2}, \quad \textbf{(3)}$$

where N_{SAMPLE} is the number of frequencies sampled by the OCM, and $P^{\text{LOW}}(f, L_S)$ and $P^{\text{HIGH}}(f, L_S)$ are the emulated power spectra at the output of the fiber span introducing for a specific set of variables, x, the measured power spectra, $P^{\text{LOW}}(f, 0)$ and $P^{\text{HIGH}}(f, 0)$, respectively. Figure 4 qualitatively represents the metrics adopted for this optimization framework. The result of this methodology is more accurate in uniform fiber condition when there are spools composing each fiber span of the same type. If this condition is not ensured, the optimization result provides equivalent parameters as if the specific fiber span were uniform.

The strong point of the proposed probing procedure relies on the identification of the fiber span physical properties operating a joint optimization of the main parameters involved within the optical fiber propagation. In addition, this approach makes it possible to produce a first classification of the in-field optical fibers without having any physical layer knowledge available.

2. Optical Line Control

The aim of the following framework is to define the optimal amplifier working point on the base of a QoT-E to maximize the OLS capacity given its physical layer description. Given the previously extracted OLS physical layer description, we address the optical line control according to two different strategies in which both of them determine the working point of each amplifier providing a mean gain, $\bar{G}$, and a gain tilt, T. In any case, these approaches depend on the introduced WDM comb spectrum, which has to be measured by the OCM at the OLS input to properly optimize the working point of the booster (BST) amplifier. The first optimization formulation
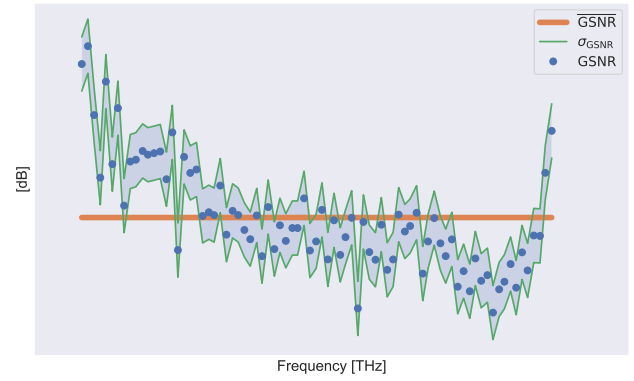
evaluates the GSNR at the output of the OLS, having a global sight of the transmission system behavior. The second one performs a set of forward optimizations starting from the BST span, one for each span and one for the pre-amplifier alone, using at the considered span input the status of the WDM comb propagated with the optimal amplifier configurations retrieved during the previous steps. Referring to the local-optimization–global-optimization (LOGO) strategy [33], this second optimization is based on a similar approach, modularizing a complex problem into smaller ones and evaluating the proportion between the two ASE and NLI noise contributions. Regarding the problem dimension, in the first case, there is a single optimization with a number of variables to optimize that is two times the number of the OLS amplifiers. In the second case, the number of optimizations is equal to the number of the OLS spans plus one related to the pre-amplifier working point, but the number of variables is fixed at two, since a single amplifier is optimized at each step.

Starting from the first optimization formulation based on the evaluation of the global GSNR, the fitness of each generated amplifier parameter configuration is evaluated as follows:

$$\max_{\bar{G}_i, T_i} \left\{ \overline{\text{GSNR}}(\bar{G}_i, T_i) - \sigma_{\text{GSNR}}(\bar{G}_i, T_i) \right\}, \quad \textbf{(4)}$$

where i is the index related to the specific amplifier, and $\overline{\text{GSNR}}(\bar{G}_i, T_i)$ and $\sigma_{\text{GSNR}}(\bar{G}_i, T_i)$ are the mean GSNR and relative standard deviation in dB units (Fig. 5), respectively.

For each step, the second local optimization formulation follows the metrics summarized in Fig. 6 and is expressed as

$$\min_{\bar{G}, T} \left\{ m_{P_{ch}} + \sum_{i=1}^{N_{ch}} P_{\text{ASE}}(f_i) - 2 \cdot P_{\text{NLI}}(f_i) \right\}, \quad \textbf{(5)}$$

where $\bar{G}$ and T are the parameters of the specific amplifier to optimize, $P_{\text{ASE}}(f)$ and $P_{\text{NLI}}(f)$ are the two noise contribution profiles at the output of the considered span in linear units also depending on the amplifier parameters, and $m_{P_{ch}}$ is the linear regression angular coefficient of the signal power profile.

The agnostic optimization approach confers to this control strategy the possibility to uniquely determine the OLS operation without adopting power sweep procedures to establish the amplifier working point. Furthermore, the proposed methodologies are effective in the case of a full spectral
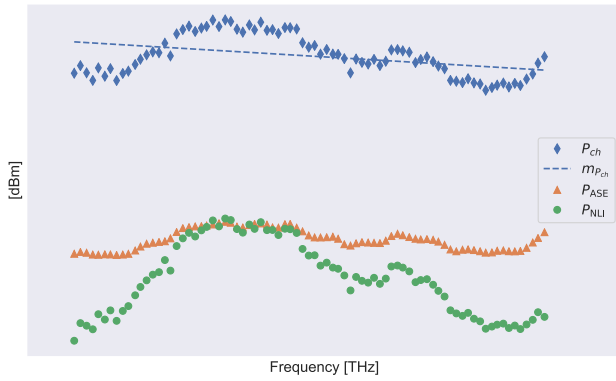
Fig. 6. Adopted metrics for *local* GSNR optimization within the optical line control strategy.

load transmission condition, having minimal variations of the introduced WDM comb and avoiding the presence of transients.

4. EXPERIMENTAL SETUP

A WDM comb composed of 80 channels centered at 193.35 THz with a WDM grid spacing of 50 GHz within the C-band is generated by manipulating an ASE noise source output with a commercial programmable WaveShaper (1000S from Finisar), obtaining a final flat spectrum with an average power level of −23 dBm. Nine independent channels under test (CUTs) over the 80 channels are chosen in order to have an equally distributed sampling of the spectrum; for these CUTs, the signal transmission is managed by a commercial AS7716-24SC Cassini device, along with a C form-factor pluggable 2 digital coherent optics (CFP2-DCO) coherent module from Lumentum, configured to generate a 32 GBaud, polarizaion-multiplexed quadrature phase shift keying (PM-QPSK) modulated signal. The same module is equipped with a coherent receiver section, followed by digital equalization and time, carrier, and phase estimation sections necessary for the signal recovery and for the pre-forward error correcting code (FEC) bit error rate (BER) evaluation. The OLS consists of eight fiber spans, each approximately 80 km long, with a mixture of single-mode fiber types, characterized by distinct physical parameters and preceded by a commercial EDFA operating with distinct and constant gain and tilt values. The sketch of the complete experimental setup is depicted in Fig. 7.
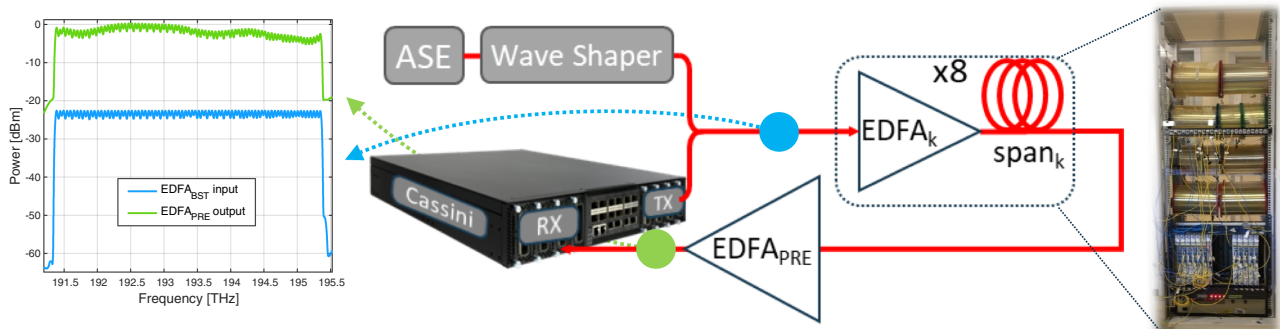
At the output of the OLS, a pre-amplifier is used to fix the channel's optical power at the receiver's input and to evaluate the CUT OSNR and the power levels of all 80 channels by means of the integrated OCM; an example spectrum power measurement performed using the OCM is shown in Fig. 7. The pre-FEC BER in transmission for each CUT is then measured by means of the CFP2-DCO coherent module. By inverting the BER versus the OSNR curve obtained through a progressive back-to-back noise loading characterization [27], we obtain a quantitative estimation of the GSNR. In this experimental proof of concept, the proper operation of the conceived architecture is investigated without automatizing with standard protocols the exchange of information between telemetry devices and the software controller. The acquisition and the sending of data are made by means of embedded laboratory protocols.

A. EDFA Characterization

A precise procedure has been applied to each EDFA to characterize the gain profile along the frequency produced by the specific device, given different values of tilt and gain targets. On the contrary, a fixed value for the NF has been considered for all the EDFAs.

In this procedure, a fixed input spectrum, including 40 channels along the C-band, is amplified setting 15 different gain targets. For each gain target, 15 different tilt targets are tested, in turn. All the output spectra are measured with an optical spectrum analyzer (OSA), and the extracted gain profiles are evaluated. These profiles can be characterized by three features: the mean gain, tilt coefficient, and residual ripple profile. In particular, the tilt coefficient is defined as the angular coefficient of the linear regression of the output spectrum profile, and, in general, it is proportional to the target tilt, as the mean gain is roughly equal to the gain target. As expected, these proportions between the observed and target values of the tilt and gain are verified up to a maximum value of output power. When this threshold is reached, the output profiles tend to a fixed, maximum, and flat profile. On the other hand, the ripple profiles vary for all the gain and tilt values, with higher fluctuations when the power out threshold is approached.

These three characterizing quantities, along with the power out threshold, are measured for all the EDFAs and used to create the software implementation that accurately reproduces these amplification procedures.

Fig. 7. Experimental setup and OCM measurements of the transmitted and received spectra.

5. RESULTS AND DISCUSSION

First, the physical layer characterization process is applied to the described experimental setup. The complete set of results is synthesized for each span in Table 1 and in Figs. 8 and 9. Starting from the extracted Raman efficiencies, which are strictly related to the fiber effective area, it is possible to operate a classification of the analyzed fibers even without knowledge of the in-field-type variety, deducing the corresponding value of dispersion.

On the basis of the reported OLS physical layer description, the OLC produces the configuration of the amplifier parameters. The mean gain ranges from 14.5 dB to 20.5 dB, and each tilt goes from -1.5 dB to 1.5 dB, referring to the C-band in frequency ($\simeq 4$ THz).

The problem dimension has a considerable impact on optimization time. In this particular case, the single optimization with 18 variables of the global control strategy takes a variable time interval of some tenths of minutes. On the other hand, the total optimization time of the nine small optimizations with two variables is less than 2 min. This time performance is achieved using a 2.2 GHz quad-core Intel Core i7 processor with a 16 GB 1600 MHz DDR3 RAM.

For both the global and local control strategies, the optimization process results of the final amplifier configurations are reported in Tables 2 and 3, respectively. As a preliminary experimental step, the receiver site penalties are properly characterized making the residual impairment comparable with measurement error. Using the optimized amplifier
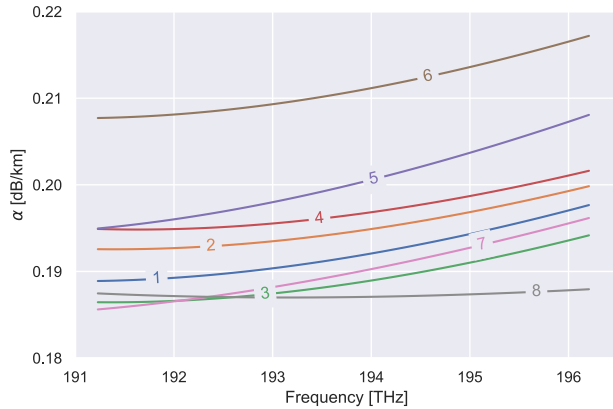
Fig. 8. Loss coefficient functions extracted during the physical layer characterization for each fiber span.
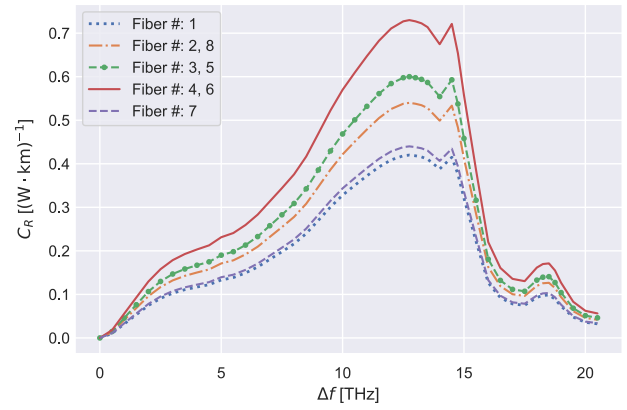
Fig. 9. Raman efficiency profiles extracted during the physical layer characterization for each fiber span.

parameter configurations, four different experiments are carried out for each control strategy modifying the BST mean gain from -2 dB to $+1$ dB with steps of 1 dB. This experimental campaign aims to demonstrate that the evaluated optimal working points are actually close to the optimum, comparing the GSNR profiles collected during this power sweep.

The two sets of experiments for both control strategies are summarized in Figs. 10 and 11. Observing the GSNR error profiles in Figs. 10(b) and 11(b), it is remarkable that, in the face of the operated physical layer characterization, GNPy estimates extremely accurately the GSNR profile for all amplifier configurations of both power sweeps. In fact, the emulations are conservative in almost all cases with a maximum error strictly below 0.9 dB. Considering the aggregated metrics, the optimized amplifier configuration derived from the global approach shows sub-optimal characteristics due to a smaller mean GSNR, 21.6 dB, and a more dispersed profile, 0.22 dB, of standard deviation, with respect to the same configuration with a BST gain set at 18.9 dB. On the other hand, the local control configuration has the lowest standard deviation, 0.13 dB, and a mean GSNR almost equal to the achieved maximum one in the power sweep and larger than that of the global control strategy, 21.9 dB. In both cases, the performance of the achieved experimental results is excellent in terms of GSNR profile flatness, bringing the system to work close to the actual global optimum. Comparing the two control strategies, the local approach is more effective in tackling the final goal, achieving a GSNR profile with a higher mean and a more

Table 1. Results of Physical Layer Characterization Procedure Performed on Each Fiber Span Composing the Experimental OLS

Span	L_S [km]	C_R [(W·km)$^{-1}$]	D [ps/(nm·km)]	$\alpha(f_{OTDR})$ [dB/km]	$l(z=0)$ [dB]	$l(z=L_S)$ [dB]
#1	80.4	0.42	16.7	0.191	0.9	0.1
#2	80.4	0.54	3.8	0.194	2.0	1.0
#3	80.6	0.60	8.0	0.188	0.6	0.3
#4	79.9	0.73	4.4	0.196	0.1	3.6
#5	79.8	0.60	8.0	0.199	0.1	2.3
#6	75.8	0.73	4.4	0.210	1.7	0.4
#7	64.7	0.44	16.7	0.189	0.2	3.0
#8	78.6	0.54	3.8	0.187	0.3	0.1

Table 2.   Amplifier Parameter Configuration Optimized Using the *Global* Control Strategy

	BST	AMP$_1$	AMP$_2$	AMP$_3$	AMP$_4$	AMP$_5$	AMP$_6$	AMP$_7$	PRE
$\bar{G}$ [dB]	19.9	17.6	19.5	17.0	19.7	19.7	17.1	19.5	16.7
T [dB]	1.5	1.5	1.4	1.4	0.3	0.4	−1.5	0.1	1.4

Table 3.   Amplifier Parameter Configuration Optimized Using the *Local* Control Strategy

	BST	AMP$_1$	AMP$_2$	AMP$_3$	AMP$_4$	AMP$_5$	AMP$_6$	AMP$_7$	PRE
$\bar{G}$ [dB]	20.3	19.6	18.0	15.6	20.3	20.3	15.7	18.4	18.4
T [dB]	1.1	1.5	1.5	1.5	1.5	1.5	1.5	1.5	0.8
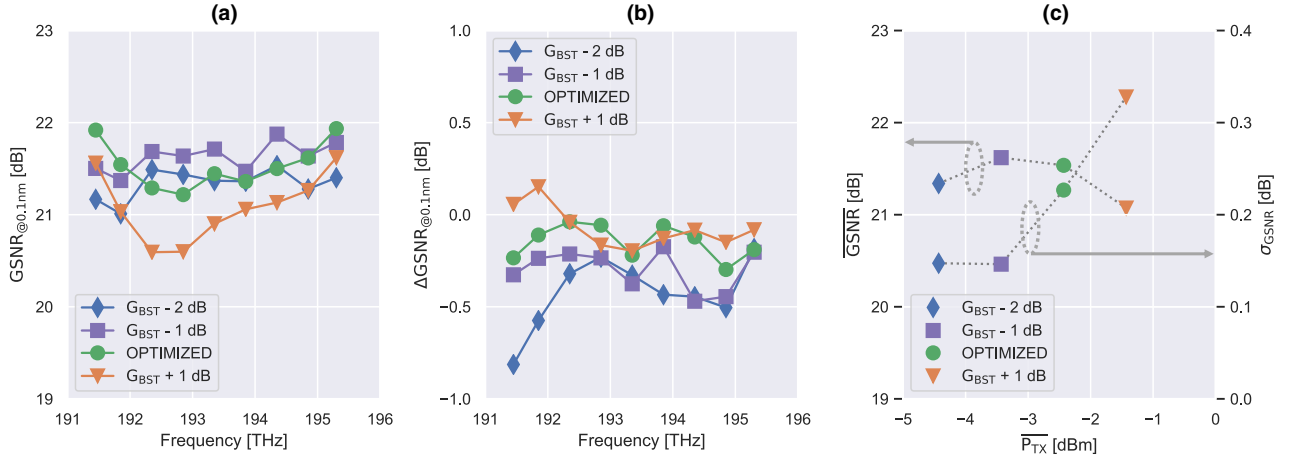
Fig. 10.   Experimental results of the *global* control strategy using a noise bandwidth of 0.1 nm: (a) GSNR profiles, (b) error profiles between GNPy emulation and experimental measurement, and (c) GSNR aggregated metrics versus the BST output power average level: mean and standard deviation.
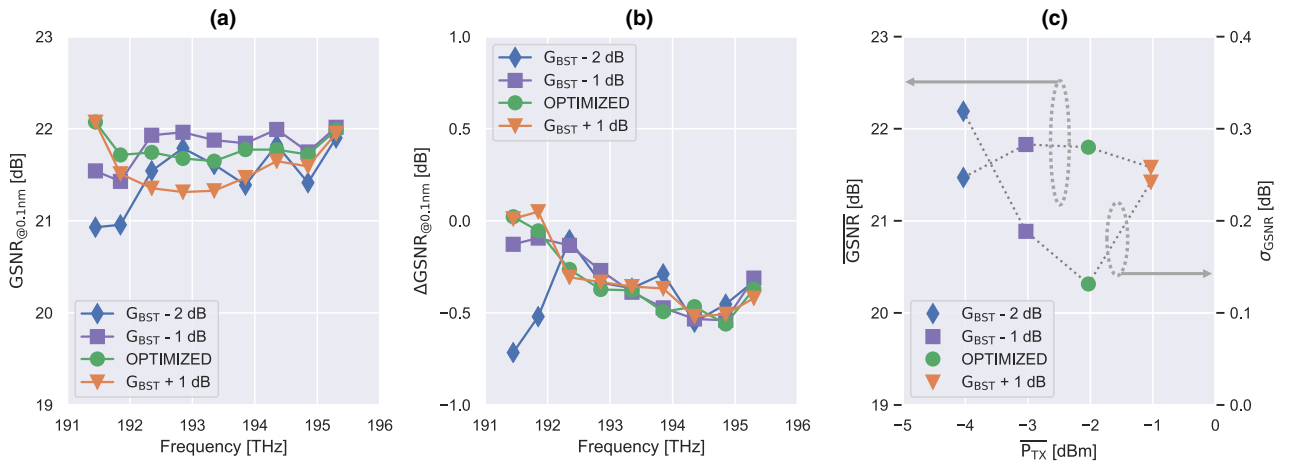
Fig. 11.   Experimental results of the *local* control strategy using a noise bandwidth of 0.1 nm: (a) GSNR profiles, (b) error profiles between GNPy emulation and experimental measurement, and (c) GSNR aggregated metrics versus the BST output power average level: mean and standard deviation.

distributed shape. It takes a noticeably small amount of time in completing the optimization process, due to the modular problem formulation with a higher number of optimizations but with a small number of variables to optimize. In addition, this framework makes it possible to accurately determine the dependency between the GSNR profile with respect to the amplifier configuration due to the forward local approach, span by span.

6. CONCLUSION

A software framework implementing a cognitive and autonomous OLC is presented and experimentally tested in the laboratory. It consists of a vendor-agnostic optimization process that determines the working point of each amplifier within the OLS to obtain the GSNR profile with the maximum average and flatness, and minimum ripple, using a faithful

OLS physical layer description. The latter is retrieved by an automatic physical layer characterization procedure that exploits the data measured by in-field monitoring devices to extract the properties of each fiber span. Two different control strategies are presented and experimentally proved, showing excellent results in terms of achieved GSNR profiles in both cases. In particular, it is observed that using a local control strategy that focuses on the QoT evaluation optimizing each amplifier working point, span by span, is more effective in terms of execution time and achieved performance than a global optimization that analyzes the GSNR at the output of the OLS. Using the physical layer information derived by the characterization process and comparing the experimental data with the emulated, it is remarkable that the GNPy physical model shows an extremely faithful and accurate QoT-E. The adopted evolutionary optimization process is a reasonable choice to tackle high-dimensional and nonlinear problem spaces such as the formulated ones, demonstrated to be significantly effective in terms of time and solution goodness.

REFERENCES

1. "Cisco visual networking index: global mobile data traffic forecast update, 2017–2022" (2019).
2. E. B. Desurvire, "Capacity demand and technology challenges for lightwave systems in the next two decades," J. Lightwave Technol. **24**, 4697–4710 (2006).
3. L. Velasco and M. Ruiz, "Optical network automation [Invited Tutorial]," in *22nd International Conference on Transparent Optical Networks (ICTON)* (IEEE, 2020).
4. M. Jinno, T. Ohara, Y. Sone, A. Hirano, O. Ishida, and M. Tomizawa, "Elastic and adaptive optical networks: possible adoption scenarios and future standardization aspects," IEEE Commun. Mag. **49**(10), 164–172 (2011).
5. D. Zhang, D. Liu, X. Wu, and D. Nesset, "Progress of ITU-T higher speed passive optical network (50G-PON) standardization," J. Commun. Netw. **12**, D99–D108 (2020).
6. C.-S. Li and W. Liao, "Software defined networks," IEEE Commun. Mag. **51**(2), 113 (2013).
7. S. Agarwal, M. Kodialam, and T. Lakshman, "Traffic engineering in software defined networks," in *IEEE INFOCOM* (IEEE, 2013), pp. 2211–2219.
8. N. Foster, A. Guha, M. Reitblatt, A. Story, M. J. Freedman, N. P. Katta, C. Monsanto, J. Reich, J. Rexford, C. Schlesinger, D. Walker, and R. Harrison, "Languages for software-defined networks," IEEE Commun. Mag. **51**(2), 128–134 (2013).
9. M. Filer, M. Cantono, A. Ferrari, G. Grammel, G. Galimberti, and V. Curri, "Multi-vendor experimental validation of an open source QoT estimator for optical networks," J. Lightwave Technol. **36**, 3073–3082 (2018).
10. M. De Leenheer, Y. Higuchi, and G. Parulkar, "An open controller for the disaggregated optical network," in *International Conference on Optical Network Design and Modeling (ONDM)* (2018), pp. 230–233.
11. R. Casellas, R. Martínez, R. Vilalta, and R. Muñoz, "Metro-haul: SDN control and orchestration of disaggregated optical networks with model-driven development," in *20th International Conference on Transparent Optical Networks (ICTON)* (IEEE, 2018).
12. F. Paolucci, A. Sgambelluri, F. Cugini, and P. Castoldi, "Network telemetry streaming services in SDN-based disaggregated optical networks," J. Lightwave Technol. **36**, 3142–3149 (2018).
13. G. S. Zervas and D. Simeonidou, "Cognitive optical networks: need, requirements and architecture," in *12th International Conference on Transparent Optical Networks* (IEEE, 2010).
14. W. Wei, C. Wang, and J. Yu, "Cognitive optical networks: key drivers, enabling techniques, and adaptive bandwidth services," IEEE Commun. Mag. **50**(1), 106–113 (2012).
15. V. W. S. Chan, "Cognitive optical networks," in *IEEE International Conference on Communications (ICC)* (2018).
16. I. de Miguel, R. J. Durán, T. Jiménez, N. Fernández, J. C. Aguado, R. M. Lorenzo, A. Caballero, I. T. Monroy, Y. Ye, A. Tymecki, I. Tomkos, M. Angelou, D. Klonidis, A. Francescon, D. Siracusa, and E. Salvadori, "Cognitive dynamic optical networks [Invited]," J. Opt. Commun. Netw. **5**, A107–A118 (2013).
17. F. Paolucci and A. Sgambelluri, "Telemetry in disaggregated optical networks," in *International Conference on Optical Network Design and Modeling (ONDM)* (IEEE, 2020).
18. G. Borraccini, S. Straullu, A. D'Amico, A. Nespola, S. Piciaccia, A. Tanzi, G. Galimberti, and V. Curri, "Autonomous physical layer characterization in cognitive optical line systems," to appear in Optical Fiber Communication Conference (OFC) 2021.
19. G. Borraccini, S. Straullu, A. D'Amico, E. Virgillito, L. Kumar, S. Piciaccia, S. Bottacchi, S. Swail, G. Galimberti, and V. Curri, "QoT-E driven optimized amplifier control in disaggregated optical networks," to appear in Optical Fiber Communication Conference (OFC) 2021.
20. J. Kundrát, O. Havliš, J. Jedlinský, and J. Vojtěch, "Opening up ROADMs: let us build a disaggregated open optical line system," J. Lightwave Technol. **37**, 4041–4051 (2019).
21. M. Birk, O. Renais, G. Lambert, C. Betoule, G. Thouenon, A. Triki, D. Bhardwaj, S. Vachhani, N. Padi, and S. Tse, "The OpenROADM initiative," J. Opt. Commun. Netw. **12**, C58–C67 (2020).
22. S. Gringeri, B. Basch, V. Shukla, R. Egorov, and T. J. Xia, "Flexible architectures for optical transport nodes and networks," IEEE Commun. Mag. **48**(7), 40–50 (2010).
23. E. Riccardi, P. Gunning, Ó. G. de Dios, M. Quagliotti, V. López, and A. Lord, "An operator view on the introduction of white boxes into optical networks," J. Lightwave Technol. **36**, 3062–3072 (2018).
24. C. Manso, R. Muñoz, N. Yoshikane, R. Casellas, R. Vilalta, R. Martnez, T. Tsuritani, and I. Morita, "TAPI-enabled SDN control for partially disaggregated multi-domain (OLS) and multi-layer (WDM over SDM) optical networks," J. Opt. Commun. Netw. **13**, A21–A33 (2021).
25. J. Kundrát, A. Campanella, E. Le Rouzic, A. Ferrari, O. Havliš, M. Hažlinský, G. Grammel, G. Galimberti, and V. Curri, "Physical-layer awareness: GNPy and ONOS for end-to-end circuits in disaggregated networks," in *Optical Fiber Communication Conference (OFC)* (Optical Society of America, 2020), paper M3Z.17.
26. V. Curri, "Software-defined WDM optical transport in disaggregated open optical networks," in *22nd International Conference on Transparent Optical Networks (ICTON)* (IEEE, 2020).
27. A. Ferrari, M. Filer, K. Balasubramanian, Y. Yin, E. Le Rouzic, J. Kundrát, G. Grammel, G. Galimberti, and V. Curri, "GNPy: an open source application for physical layer aware open optical networks," J. Opt. Commun. Netw. **12**, C31–C40 (2020).
28. A. Ferrari, K. Balasubramanian, M. Filer, Y. Yin, E. le Rouzic, J. Kundrát, G. Grammel, G. Galimberti, and V. Curri, "Softwarized optical transport QoT in production optical network: a Brownfield validation," in *European Conference on Optical Communications (ECOC)* (2020).
29. J. Bromage, "Raman amplification for fiber communications systems," J. Lightwave Technol. **22**, 79–93 (2004).
30. N. Hansen, S. D. Müller, and P. Koumoutsakos, "Reducing the time complexity of the derandomized evolution strategy with covariance matrix adaptation (CMA-ES)," Evol. Comput. **11**, 1–18 (2003).
31. N. Hansen, Y. Akimoto, and P. Baudis, "CMA-ES/pycma on Github," Zenodo (2019), https://doi.org/10.5281/zenodo.2559634.
32. S. Walker, "Rapid modeling and estimation of total spectral loss in optical fibers," J. Lightwave Technol. **4**, 1125–1131 (1986).
33. P. Poggiolini, G. Bosco, A. Carena, R. Cigliutti, V. Curri, F. Forghieri, R. Pastorelli, and S. Piciaccia, "The LOGON strategy for low-complexity control plane implementation in new-generation flexible networks," in *Optical Fiber Communication Conference and the National Fiber Optic Engineers Conference (OFC/NFOEC)* (Optical Society of America, 2013), paper OW1H.3.